Chemistry and Physics of Lipids 225 (2019) 104816

Contents lists available at ScienceDirect

Chemistry and Physics of Lipids

journal homepage: www.elsevier.com/locate/chemphyslip

The effect of hydrophilic penetration/diffusion enhancer on stratum corneum lipid models: Part II*: DMSO*

J. Mueller[a], M. Trapp[b], R.H.H. Neubert[c,*]

[a] Department of Pharmaceutics and Biopharmaceutics, Institute of Pharmacy, Martin Luther University Halle-Wittenberg, Wolfgang-Langenbeck-Str. 4, 06120, Halle, Germany

[b] Institute Soft Matter and Functional Materials, Helmholtz-Zentrum-Berlin für Materialien und Energie GmbH, Hahn-Meitner-Platz 1, 14109, Berlin, Germany

[c] Institute of Applied Dermatopharmacy, Martin Luther University Halle-Wittenberg, Weinbergweg 23, 06120, Halle, Germany

ARTICLE INFO

Keywords:
DMSO
Penetration/diffusion enhancer
Interactions with stratum corneum lipid model systems
Dermal and transdermal drug delivery
Mode of action

ABSTRACT

To optimize dermal and transdermal administration of drugs, the barrier function of the skin, particularly the stratum corneum (SC), needs to be reduced reversibly. For this purpose, penetration/diffusion enhancers such as DMSO can be applied. However, there is the question whether DMSO is an aggressive penetration/diffusion enhancer in pharmaceutical and cosmetical relevant concentrations? Until now, it is unclear if this penetration/diffusion enhancement is caused by an interaction with the SC lipid matrix or related to effects within the corneocytes. Therefore, the effects of the hydrophilic enhancer DMSO on SC models with different dimensionality ranging from bilayers (liposomes) via oligo-layers to multilayers have been investigated in this study. The effects of DMSO should be compared to that of other relevant hydrophilic enhancers such as urea and taurine. An innovative spectrum of methods was applied to ascertain the mode of action of DMSO in relevant concentrations on a molecular scale.

The experiments reveal that there is no specific interaction of 10% and 30% DMSO solutions with the SC model systems. Hence, if DMSO is applied in pharmaceutically and cosmetically relevant concentrations, it has no influence on the SC model systems used. Neither an additional water uptake in the head group region nor a decrease of the lipid chain packing density have been observed. The leakage studies on liposomes show that 10% DMSO is causing just a very slight leakage of 8%, lower than the leakage of 19.4% caused by 10% urea (Müller et al., 2016). Consequently, the interactions of DMSO with the SC model lipids used are very low in concentrations of 10% and 30%, respectively. Since the lipid composition in native SC lipid matrix is far more complex than this model mixture, the results can not be directly transferred to the native SC lipid matrix. However, the outcome of this study, together with various findings in the literature give rise to the assumption that the enhancing effect of DMSO concerning the diffusion of relevant hydrophilic drugs and actives appears to be realized via the corneocytes.

1. Introduction

The stratum corneum (SC) is the outermost layer of the human skin and is responsible for the strong barrier function against external influences as well as the resistance against the penetration and permeation of relevant actives and drugs. The basis of this barrier function is the structure of the SC, composed of corneocytes which are embedded in a lipid matrix according to the “brick and mortar” model (Elias, 1983). The dead corneocytes represent the bricks. On the other hand the highly ordered multilamellar lipid matrix is described as mortar representing the so called lipophilic penetration pathway substances (Boddé et al., 1991; Talreja et al., 2001; Schmitt and Neubert, 2018). The highly ordered multilamellar arrangement of the SC lipids has a very unique composition, containing ceramides (CER), free fatty acids (FFA) and cholesterol (CHOL) in a nearly equimolar ratio (Lampe et al., 1983; Law et al., 1995; Melnik et al., 1989; Wertz and van den Bergh, 1998) hindering the drugs to overcome the SC and resulting in a very low bioavailability. Therefore, penetration enhancers, which reduce the skin barrier by loosening the SC lipid structure reversibly, are used to obtain reasonable dermal and transdermal bioavailabilities. These penetration enhancers are applied to influence either hydrophilic or lipophilic pathways across the SC. Whereas the influence of lipophilic

* Part I: Biochim Biophys Acta 2016, 1858, 2006–2018.

* Corresponding author.
E-mail address: reinhard.neubert@pharmazie.uni-halle.de (R.H.H. Neubert).

https://doi.org/10.1016/j.chemphyslip.2019.104816
Received 9 June 2019; Received in revised form 28 August 2019; Accepted 3 September 2019
Available online 13 September 2019
0009-3084/

penetration enhancers on the lipophilic penetration pathway is well studied (Trommer and Neubert, 2006) the influence of hydrophilic penetration enhancers is not well understood on a molecular level. One way of the influence of hydrophilic penetration enhancers could be the interaction with the lipid head group region by loosening hydrogen bonds. As a result, the distance between adjacent bilayers increases, facilitating the penetration potential for hydrophilic drugs (Hikima and Maibach, 2006). This change in the bilayer distance may also influence the lipid chain region, causing a penetration enhancement for lipophilic drugs (Kalbitz et al., 1996). However, these mechanisms on a molecular scale are not completely understood.

DMSO is one of the first and an intensively studied hydrophilic penetration/diffusion enhancer having a log $P_{octanol/water} = -1.35$ (Hansch et al., 1995). DMSO is able to influence both the penetration of lipophilic actives and drugs as well as the diffusion of hydrophilic ones (Maibach and Feldmann, 1967; Coldman et al., 1971). According to Dragicevic et al., 2015, the influence of DMSO is based on the following mechanisms: (i) change of the intracellular keratin conformation from the alpha helical one to beta sheet one (Oertel, 1977; Anigbogu et al., 1995; Mendelsohn et al., 2006;), (ii) extraction of lipids (Allenby et al., 1969) together with formation of pores, (iii) increased partition of the drug into the skin from the formulation due to DMSO accumulated in the SC (Williams and Barry, 2012), (iv) interaction with the SC lipids, particularly, with the head groups; however, interactions of DMSO with the lipophilic chains are also possible.

The high degree of order of the SC lipids can be reduced by replacing water by DMSO molecules because the solvate shell is increased by DMSO (Guillard et al., 2009; Barry, 1987). There are just very few references in the literature dealing with the interactions of DMSO with the SC lipids. An influence of DMSO on the head groups of synthetic CER[NS] has been identified by Guillard et al., 2009. Furthermore, it is described in the literature that high concentrations of DMSO (60%) are necessary in order to achieve a penetration enhancement (Anigbogu et al., 1995; Barry, 1987; Notman et al., 2008) and a disordering and fluidisation of the acyl chains of the SC lipids (Kwak and Lafleur, 2009), respectively.

For an objective evaluation of the use of DMSO as diffusion/penetration enhancer in dermatopharmaceutics and cosmetics, respectively, systematic and comprehensive studies, focusing on the characterization of the interactions of DMSO with the SC lipids on a molecular level, are highly needed.

Therefore, the objective of this study was to characterize the influence of the hydrophilic penetration enhancer dimethyl sulfoxide (DMSO) on the SC lipid structure on a molecular scale in pharmaceutical and cosmetical relevant concentrations. Mixtures of the synthetic lipids CER[AP], CHOL and stearic acid (SA), representing a simple model of the components in the native SC lipid matrix, were used for this purpose. This enables a direct extrapolation of detected effects on single lipid species as it would not be possible using complex mixtures (Kiselev et al., 2005; de Jager et al., 2004, 2005, Engelbrecht et al., 2012). Furthermore, these simple models can provide a better indication of the influence of different factors like temperature, humidity or penetration enhancers (Engelbrecht et al., 2011, 2012; Zbytovska et al., 2009).

CER[AP] was used as model CER out of 19 ceramide subclasses which are known presently (t`Kind et al., 2012). It has been chosen because of its large number of 4 OH groups in the CER head group region. Hence, it was expected to have stronger interactions with hydrophilic penetration enhancers than other CER species, and these interactions might be detected more significantly. SA has been used as free fatty acid component because of its chain length, matching the one of CER[AP]-C18:18. This SC model lipid system in a comparable composition was used as reference system in a lot of publications, where it has been investigated with respect to the lipid assembly, for example Kiselev et al., 2007; Schroeter et al., 2009a; Schroeter, et al., 2009b; Kessner et al., 2008.

According to commonly used amounts of DMSO marked products, DMSO in an aqueous medium was added to the respective lipid models in relevant concentrations of 10 and 30% as well as of a higher one (50%). In order to consider as many different aspects as possible, different model systems were used such as ***bilayer, oligolayer*** and ***multilayer.*** Multilayers enable a lipid assembly which is representative for the SC lipid matrix, whereas oligolayer (2–15 bilayers) are even more realistic as model system, since the lipid matrix in native SC contains up to 20 bilayers. Furthermore, the reduced sample thickness enables a more sensitive detection of changes induced for example by penetration enhancers (see Fig. 1-SI..

These model systems were investigated using several appropriate methods. The spectrum of methods provides comprehensive information about the interaction mechanism of the studied enhancer DMSO on the SC lipid model systems used. The effects of DMSO on these model systems should be compared to the influence of other relevant hydrophilic enhancers such as urea and taurine.

2. Materials

CER[AP]-C18:18 (N-(α-hydroxyoctadecanoyl)-phytosphingosine) was kindly provided by Evonik Industries AG (Essen, Germany) and purified using column chromatography. CHOL (99%), SA (≥99.5%), polyethylenimine (PEI) (50% (w/v)), deuterium oxide (D_2O, purity ≥99.9 atom % D), tris(hydroxymethyl)aminomethane (TRIS) (≥99.9%), DMSO (≥99.5%), ethylenediaminetetraacetic acid (EDTA) (≥99.4%), sodium chloride (≥99.5%), 6-CF (≥95%), ammonium hydroxide and hydrogen peroxide were purchased from Sigma Aldrich GmbH (Taufkirchen, Germany). Chloroform (≥99.9%) and Triton X 100 and were obtained from Carl Roth GmbH (Karlsruhe, Germany) and methanol (≥99.9%) from VWR Chemicals (Fontenay-sous-Bois, France). Sephadex G-50 was purchased from MP Biomedicals (Santa Ana, CA, United States). Polycarbonate membranes with a pore size of 100 nm were acquired from Avanti Polar Lipids (Hamburg, Germany). Zink selenide crystals for IR measurements on multilayers were provided by Thermo Fisher Scientific Inc. (Dreieich, Germany). For simultaneous NR and IR measurement disc-shaped silicon wafers with a diameter of 60 mm and a thickness of 10 mm from Sil'Tronix (Archamps, France) were used. On two opposing ends these wafers are inclined in an angle of 45°. The wafers are polished on both sides as well as the inclined surfaces and have a RMS roughness of less than 5 Å. For fluorescence measurements quartz crystal cuvettes with 4 clear sides and 10 mm path length from Hellma Analytics (Müllheim, Germany) were used. Photon correlation spectroscopy measurements were carried out using disposable PMMA cuvettes with a filling volume of 1.5 ml from Brand (Wertheim, Germany). MilliQ water with a specific resistance of 18.2 MΩ ∗ cm was obtained, using a MilliQ purification system.

3. Model systems and methods

For all model systems a lipid composition of CER[AP], CHOL and SA in a molar ratio of 1:0.7:1 was used. In native SC, these lipids occur in a nearly equimolar ratio (Kiselev et al., 2007). However, this amount of CHOL cannot be completely incorporated into the lipid membrane (Bouwstra et al., 2000; Norlen, 2001). Therefore, it was decided to slightly decrease the CHOL amount. The model systems are shown in Fig. 1-SI in the Supporting information.

3.1. Multilayer

A solution of the lipid mixture with a concentration of 1 mg ml^{-1} was prepared, using stock solutions of these components in pure chloroform (CHOL & SA) or a mixture of chloroform and methanol (2:1) (CER[AP]). 0.545 ml of this lipid mixture were sprayed by airbrush onto a zinc selenide crystal surface at a constant flow without heating.

3.1.1. Infrared spectroscopy

Measurements were performed at the IR Spectrometer IFS 28 (Bruker Optik GmbH, Karlsruhe, Germany). The measuring unit (Foundation Series by Thermo Spectra-Tech), topped by a zinc selenide crystal with a Fresnel grinding, was temperature controlled at 35 °C. A deuterated triglycine sulphate (DTGS) detector was used to measure the resulting signal. The IR absorbance was recorded dependent on the wavenumber in the range of 680 – 4000 cm^{-1} using OPUS 4.2 software (Bruker Optik GmbH, Karlsruhe, Germany) with a resolution of about 2 cm^{-1}. 32 scans were combined to one spectrum and all spectra were corrected for the respective background. The ATR crystal was placed in a Teflon cell with a reservoir of about 0.4 ml to enable the deposition of a water phase above the SC model lipids. Firstly, the lipids were measured against pure water for 24 h to equilibrate the sample. Afterwards the water phase was replaced by the enhancer solution in water and measured again for 24 h. Experiments were performed 3 times on individually prepared samples. For data analysis peaks of the obtained spectra were fitted by a Gaussian function to determine relevant peak positions. Examples of the IR spectra are shown in Fig. 2-SI in the Supporting informations.

3.2. Oligo-layer

Oligolamellar lipid models were prepared according to the procedure, developed by Mueller et al. (2016). Therefore, RCA-1 cleaned silicon wafers, covered by a polyethylenimine layer were used. Subsequently, following the procedure developed by Mennicke and Salditt (2002), 3.5 ml of the lipid mixture with a concentration of 3.5 mg ml^{-1} was deposited by spin coating (spin-coater model: 6708D, SCS, US) at a rotation speed of 4000 rpm. The prepared sample was mounted in a flow-through cell with a volume of 2–3 ml and exposed to either pure D_2O or 10% (w/w) as well as 30% (w/w) DMSO in D_2O.

3.2.1. Simultaneous infrared and neutron reflectivity (BioRef)

NR measurements were performed at the time-of-flight reflectometer BioRef at the Helmholtz-Zentrum Berlin (HZB) (Strobl et al., 2011). A chopper speed of 25 Hz allowed to cover a scattering vector Q range from 0.007 to 0.4 $Å^{-1}$ with three angular settings (θ = 0.5°, 1.0° and 2.8°, respectively. Q is dependent on the wavelength λ and the scattering angle θ ($Q= 4\pi \sin(\Theta)/\lambda$ $Q= 4\pi \sin(\Theta)/\lambda$). A constant wavelength resolution $\Delta\lambda/\lambda$ was achieved by operating the frame defining choppers in “optical blind” mode (van Well, 1992). In the experiments described here $\Delta\theta/\theta$ was set to 5% with the angular resolution $\Delta\theta/\theta$ adjusted accordingly. The Q resolution, $\Delta Q/Q$, of the instrument can be calculated by

$$\frac{\Delta Q}{Q} = \sqrt{\left(\frac{\Delta\lambda}{\lambda}\right)^2 + \left(\frac{\Delta\theta}{\theta}\right)^2} \text{ and was thus 7 \%.}$$

The reflected neutrons were recorded in $\theta/2\theta$ geometry by a position sensitive area detector (PSD) with active area of 300 x 300 mm^2 filled with 3He. Measuring times were 3.75 h for samples exposed to D_2O. The neutron footprint on the sample was adjusted by diaphragms in the incident beam for each angle such as to avoid over-illumination of the sample.

A Bruker Vertex 70 FT-IR spectrometer (Bruker Optik GmbH, Karlsruhe, Germany) was mounted at the sample position of the instrument in order to allow for simultaneous recording of NR and ATR-FTIR spectra (Strobl et al., 2011) 128 scans were summed up for each measurement. The spectral resolution of the spectrometer was set to 2 cm^{-1}. A nitrogen cooled mercury cadmium telluride (MCT) detector was used. IR spectra in the range of 1000 to 6000 cm^{-1} were obtained using the OPUS 6.5 software package (Bruker Optik GmbH, Karlsruhe, Germany). Data analysis of the IR spectra has been carried out as described for multilayers.

Data analysis of NR curves:

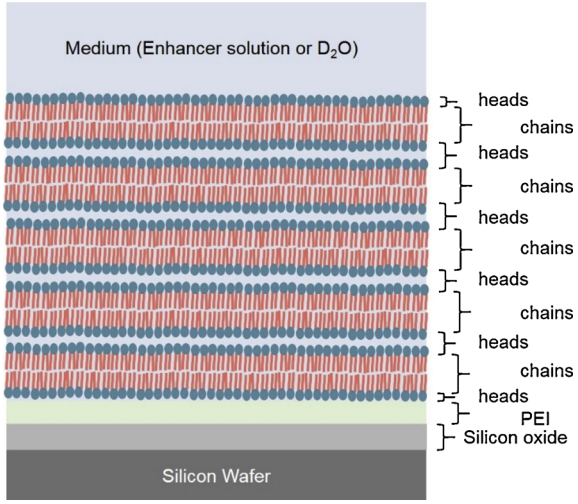

Fig. 1. Lipid model used for data analysis via optical matrix method in Motofit. Directly onto the silicon oxide layer there is a PEI anchor layer, where the 5 SC lipid bilayers are attached to. The surrounding medium is either pure D_2O or DMSO in D_2O.

Peak analysis: Peaks of the NR curves have been fitted to a Gaussian function to determine the peak maximum. Applying Bragg‘s law the spacing between adjacent Kiessig maxima provides information about the overall sample thickness via the following equation? ? = 2??/ ??????????????????.

Optical matrix method: To further investigate NR curves with respect to information about thickness and roughness of each lipid bilayer or the amount of infiltrated surrounding medium, the experimental reflectivity curves were analyzed applying a standard fitting routine in Motofit (IgorPro 6.3 Software Packet (Wavemetrics, OR)) following the method according to Abeles (Heavens, 1960; Born and Wolf, 2000). Therefore, a 13 layer model composed of 5 bilayers, as shown in Fig. 1, has been used. SLDs of the SC lipid mixture have been calculated to $1.37*10^{-6}$ $Å^{-2}$ for heads and $-0.25*10^{-6}$ $Å^{-2}$ for tails. During fitting SLDs have been fixed but the amount of medium, thickness and roughness for each layer have been fitted successively until the lowest Chi^2 has been reached.

3.3. Unilamellar liposomes (ULVs)

6-CF loaded vesicles were prepared according to Protocol 1 (Torchilin and Weissig, 2003) for the preparation of hand-shaken multilamellar lipid vesicles including some leakage specific adaptions following instructions of Blumenthal et al., 1977. Therefore, 10 mg/ml stock solutions of each component in pure chloroform (CHOL & SA) or in chloroform/methanol (2:1) (CER[AP]) were prepared and the respective amounts of each component transferred into a round bottom flask. The solvent was removed, using a rotary evaporator and the films were kept under vacuum over night to remove all remaining solvent molecules. The dry films were suspended in Tris buffer (10 mM + 100 mM NaCl, pH 10) to a concentration of 1 mg/ml. For leakage measurements the buffer solution additionally contains 50 mM 6-CF. As already examined by Zbytovská et al., 2008, the high pH value of 10 is necessary to ensure a prolonged stability of the ULVs, since at physiological pH the liposomes are more unstable and thus complicate data analysis (Zbytovska, 2006). Furthermore, test measurements showed no significant influence of the pH on the investigated properties at 32 °C. The formed suspensions were kept in a drying oven for 1 h at a temperature of 90 °C and vortexed every 30 min, which results in multilamellar vesicles (MLVs). Afterwards, the hot suspension of MLVs was extruded 21 times through a polycarbonate membrane of 100 nm pore size using a Mini extruder from Avanti Polar Lipids (Hamburg,

Germany) to produce ULVs. In case of leakage measurements, size exclusion chromatography through a Sephadex G-50 column with isosmotic Tris buffer (10 mM, pH 10) as the eluent was applied to separate the liposome incorporated 6-CF from the 6-CF of the outer water phase.

3.3.1. 6-Carboxyfluorescein leakage

Fluorescence measurements to determine the 6-CF leakage were performed at the FluoroMax – 2 of Instruments S.A., Inc., JOBIN YVON/SPEX Division (Edison, New Jersey, USA), according to previous leakage studies on phospholipid systems (de la Maza and Parra, 1996); Nishijo et al., 2000). The sample temperature of 32 °C was controlled by a circulating water bath. As excitation wavelength 485 nm was used and the respective fluorescence intensity at 520 nm was recorded using the software ISA. 10 µl of the separated liposomes were added to 2.7 ml Tris buffer in a quartz cuvette and measured subsequently to determine the initial leakage (I_o) of the sample. 300 µl DMSO were added during the fluorescence measurement to a total concentration of 10% (w/w) in buffer and measured for at least 5 min. Afterwards, 100 µl of a 20% (v/v) Triton X solution in water were added to determine the 100% leakage value. All intensities have been corrected for variations in volume and the 6-CF leakage for each time point t has been determined according to

$L(t) = \frac{I_{(t)} - I_0}{I_{100} - I_0}$ (de la Maza and Parra, 1996). The enhancer was tested 3 times. For concentrations of 30% and 50% (w/w) DMSO the initial amount of buffer as well as the amount of DMSO solution added have been adapted accordingly.

3.3.2. Photon correlation spectroscopy

PCS measurements were performed with the Zetasizer Nano ZS from Malvern Instruments Ltd (Malvern, UK) 3 times on individually prepared samples. The z-average and the PDI were calculated using the Zetasizer Software 7.03. During stability measurements, the samples were stored at 8 °C.

4. Results and discussions

4.1. Multilayer

Initially, IR measurements were carried out using SC multilayers and a pharmaceutically relevant solution of 10% DMSO. The corresponding peak positions of the three samples are shown in Table 1. No distinct effects were measured for 10% of DMSO. Therefore, a higher concentration of 50% DMSO was applied. The data are also given in Table 1.

The peak position of the amide II group has not changed, indicating that the hydrogen bonds related to the N—H group of CER[AP] are not influenced by DMSO. However, the wave number of the amide I band of the less hydrogen-bonded species at ~1640 cm^{-1} increased with higher DMSO concentrations. The peak position of the highly hydrogen-bonded species at ~1620 cm^{-1} was not influenced. In accordance with the studies of (Guillard et al., 2009) it can be stated that DMSO causes a decrease in hydrogen bonding for the less hydrogen-bonded species related to the C = O-group of CER[AP]. This effect is more prominent at higher DMSO concentrations and probably caused by the replacement of water molecules by DMSO molecules. For the highly hydrogen-bonded species no influence was obtained even at a DMSO concentration of 50%. Possible reasons for this effect could be (i) that the ratio enhancer /lipid is too low or (ii) DMSO is not able to influence these hydrogen bonds. In contrast, the wave numbers of the carbonyl stretch vibration (ν(CO)) in the range of 1700 to 1720 cm^{-1} increase with increasing DMSO concentrations, caused by the weakening of the hydrogen bond network of SA.

The positions of the asymmetric and symmetric CH_2 stretching bands (ν_{as} (CH_2) and ν_s (CH_2)), as well as the CH_2 scissoring band ($\delta(CH_2)$) at ~1466 cm^{-1}, are not influenced neither by 10% nor by 50% DMSO. Therefore, there is no influence of DMSO on the packing of the CH_2 chains. The CH_2 chains have a hexagonal chain packing.

4.2. Oligolayer

Initially, simultaneous IR and NR measurements on oligolayers were performed using a DMSO concentration of 10% where just slight changes were detected. Therefore, the DMSO concentration was increased to 30%. A concentration of 50% DMSO was not used in order to prevent an interfacial unbonding of the oligo-lipid layers.

In contrast to IR studies on multilayers, 10% and 30% DMSO did not influence the peak positions of the asymmetric and symmetric CH_2 stretching vibrations (see Table 2). However, the position of the Amide I peak which was influenced on the multilayers by DMSO had just a very weak signal and could not be clearly determined.

The NR curves for the simultaneously carried out neutron reflectivity (NR) measurements against D_2O and 10% DMSO are shown in Fig. 2 (grey and light red squares). The total thickness of the lipid layer against D_2O has been calculated by peak analysis to 163.4 ± 4.2 Å and

Table 1
Characteristic IR peak positions [cm^{-1}] of a multilamellar SC lipid model (CER[AP]: CHOL: SA) measured against water and against 10% and 50% DMSO, respectively. The positions of weak peaks were not determined (n.d.).

peak	sample 1			sample 2			sample 3		
	H_2O reference	DMSO 10 %	DMSO 50 %	H_2O reference	DMSO 10 %	DMSO 50 %	H_2O reference	DMSO 10 %	DMSO 50 %
ν_{as} (CH_2)	2914.9 ± 0.1	2914.8 ± 0.1	2914.9 ± 0.1	2915.4 ± 0.1	2915.4 ± 0.1	2915.4 ± 0.1	2914.8 ± 0.1	2914.8 ± 0.1	2914.8 ± 0.1
ν_s (CH_2)	2848.7 ± 0.1	2848.7 ± 0.1	2848.7 ± 0.1	2849.0 ± 0.1	2848.9 ± 0.1	2849.0 ± 0.1	2848.6 ± 0.1	2848.6 ± 0.1	2848.6 ± 0.1
ν(CO)	1722.1 ± 0.2	1722.2 ± 0.2	1722.9 ± 0.1	1723.4 ± 0.1	1723.6 ± 0.2	1723.7 ± 0.2	1723.3 ± 0.2	1723.4 ± 0.1	1723.3 ± 0.2
	1700.4 ± 0.2	1700.6 ± 0.1	1701.7 ± 0.1	n.d.	n.d.	n.d.	n.d.	n.d.	n.d.
Amide I	1638.4 ± 0.1	1638.7 ± 0.1	1639.2 ± 0.1	1638.2 ± 0.2	1638.7 ± 0.2	1639.1 ± 0.2	1638.8 ± 0.2	1639.6 ± 0.2	1639.6 ± 0.2
	1620.0 ± 0.1	1619.9 ± 0.1	1619.8 ± 0.1	1620.3 ± 0.1	1620.2 ± 0.1	1620.0 ± 0.1	1619.3 ± 0.1	1619.3 ± 0.1	1619.2 ± 0.1
Amide II	1540.3 ± 0.1	1540.4 ± 0.1	1540.5 ± 0.1	1540.9 ± 0.1	1540.8 ± 0.1	154.8 ± 0.1	1540.4 ± 0.1	1540.4 ± 0.1	1540.4 ± 0.1
$\delta(CH_2)$	1466.2 ± 0.1	1466.2 ± 0.1	1466.2 ± 0.1	1466.1 ± 0.1	1466.1 ± 0,.1	1466.1 ± 0.1	1466.3 ± 0.1	1466.3 ± 0.1	1466.3 ± 0.1

Table 2
IR peak positions [cm^{-1}] of the oligolamellar SC lipid model (CER [AP]:CHOL:SA) against D_2O as well as 10% and 50% DMSO in D_2O.

Peak	D_2O reference	DMSO 10 %	DMSO 30 %
$\nu_{as}(CH_2)$	2917.9 ± 0.2	2917.9 ± 0.3	2917.9 ± 0.1
$\nu_s(CH_2)$	2850.2 ± 0.2	2850.2 ± 0.3	2850.1 ± 0.1

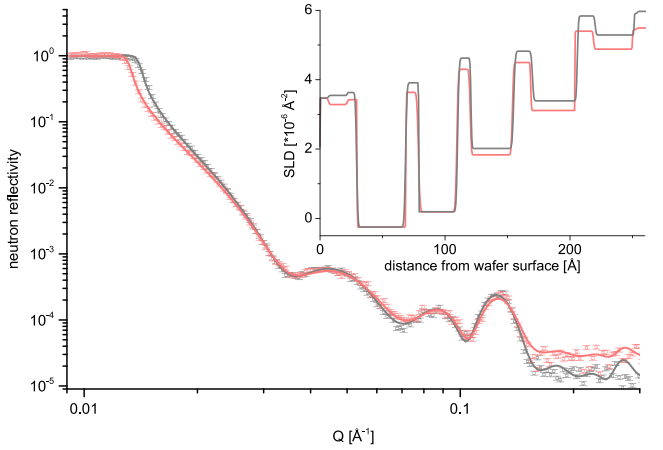

Fig. 2. Neutron reflectivity curves of an oligolamellar sample (CER [AP]:CHOL:SA), measured against D_2O (grey squares) and subsequently against 10% DMSO in D_2O (light red squares). The corresponding fits are presented as lines of the same color and the corresponding scattering length density profiles are given in the inset.

increased slightly but not significantly to 166.5 ± 4.4 Å after addition of 10% DMSO. The positions of the Bragg peaks show a slight shift from 0.1297 ± 0.0002 $Å^{-1}$ in D_2O to 0.1304 ± 0.0002 $Å^{-1}$ against 10% DMSO, possibly indicating a changed layer thickness.

To further investigate this observation, an optical matrix analysis was applied where the experimental NR curves were fitted to the most probable theoretical curve (see Fig. 2, grey and light red lines). The corresponding scattering length density (SLD) profile of the D_2O-reference system shows already for water characteristic five layer structure with decreasing degree of coverage (Fig. 2, inset: grey line). The NR curve just slightly changed after addition of 10% DMSO in D_2O. In the corresponding SLD profile (Fig. 2, inset: light red line) there is a decrease of the SLD in each layer, reasoned by the lower SLD of the medium which additionally contains DMSO. Furthermore, the amount of medium in the outer lipid layers tends to increase as indicated by the data shown in Table 3. Since the data do not show any changes in the

Table 3
Thickness of the layers [Å] and amount of the medium in each layer [%] according to the SLD profiles from Fig. 2 and Fig. 3.

	D_2O		DMSO 10 %		DMSO 30 %	
	thickness	medium	thickness	medium	thickness	medium
wafer						
heads	7.5	49.2	8.0	49.9	7.1	39.9
chains	39.2	0.02	39.0	0.02	34.9	0.12
heads	10.5	55.3	10.0	55.0	12.2	64.9
chains	31.2	7.1	30.7	7.7	31.8	6.9
heads	10.6	70.8	10.7	71.2	14.8	74.6
chains	34.2	364	33.8	36.3	32.1	31.8
heads	14.9	75.0	14.7	75.9	15	84.8
chains	36.0	58.5	35.5	58.6	30.4	53.6
heads	14.,3	97.1	14.8	97.8	14.8	96.9
chains	31.1	89	31.1	89.4	32.5	88.5
heads	2.6	98.6	3.1	98.7	5.7	98.9
medium						

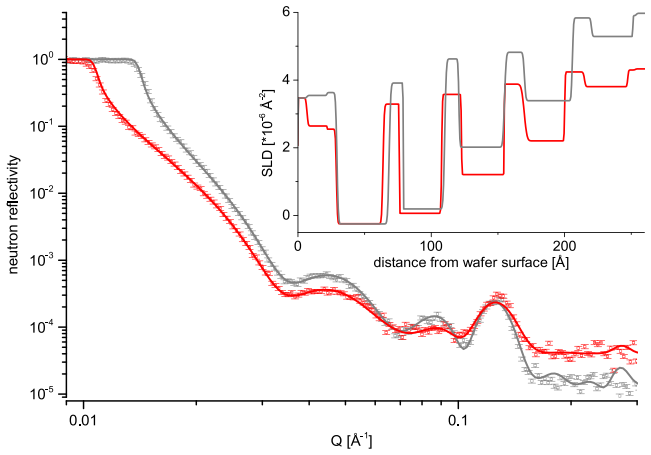

Fig. 3. Neutron reflectivity curves of an oligolamellar sample (CER [AP]:CHOL:SA), measured against D_2O (grey squares) and subsequently against 30% DMSO in D_2O (red squares). The corresponding fits are presented as lines of the same color and the corresponding scattering length density profiles are given in the inset.

layer thickness or composition, this might be caused by a slight detachment/solubilization of the lipids. Beyond that, there are no changes in the profile.

A significantly increased total thickness of the lipid layer of 172.9 ± 4.8 Å has been calculated after addition of 30% DMSO using peak analysis. Additionally, a further shift of the position of the Bragg peak to 0.1318 ± 0.0003 $Å^{-1}$ was obtained. The fits of the NR curves and the corresponding SLD profiles also show distinct differences (see Fig. 3 and Table 3).

A strong decrease of the SLD was observed in the range of the head groups and in the external chain layers. This is partly reasoned by the medium itself, as the resulting SLD of the medium is distinctly lower than the SLD of D_2O because DMSO has a SLD of about -0.04*10^{-6} $Å^{-2}$ and D_2O of about 6.36*10^{-6} $Å^{-2}$. The changes in the amount of medium in each layer are shown in Table 3 after addition of a solution of 30% DMSO. As shown there, the percentages of the medium in the range of the head groups tend to increase, probably caused by accumulation of a DMSO/D_2O mixture in this range.

The replacement of water by DMSO as described in the literature (Guillard et al., 2009; Barry, 1987) could not be confirmed using this lipid model. In this case, a decrease of the percentage of the medium must have been observed, because a decrease of the SLD of this layer would be caused by the displacement of D_2O. Additionally, a solubilization of a small part of the lipids in the outer lipid layers, as already described for 10% DMSO, might have been occurred. However, this effect could not be shown by the data, probably being superimposed by the enrichment of the DMSO solution. For the total thickness of the lipid layer no significant change could be observed using the optical matrix method, whereas with peak analysis an increased total thickness was calculated. Here, the results from peak analysis are more reliable, since they are based on the real NR curve, while optical matrix method values are based on the fit.

4.3. Liposomes

Photon correlation spectroscopy (PCS) measurements after storage in 10% DMSO show that the unilamellar vesicles/liposomes (ULV) are relatively stable over a period of eight days. Initially, the liposomes had a diameter of 145.2 ± 0.9 nm, whereas the dimensions of the liposomes in buffer had been 129.1 ± 1.0 nm (see Fig. 4a). This could be explained by the incorporation of DMSO molecules into the lipid head groups during the preparation as already described for the enhancer taurine (see Müller et al., 2016). Within eight days, the diameter of the

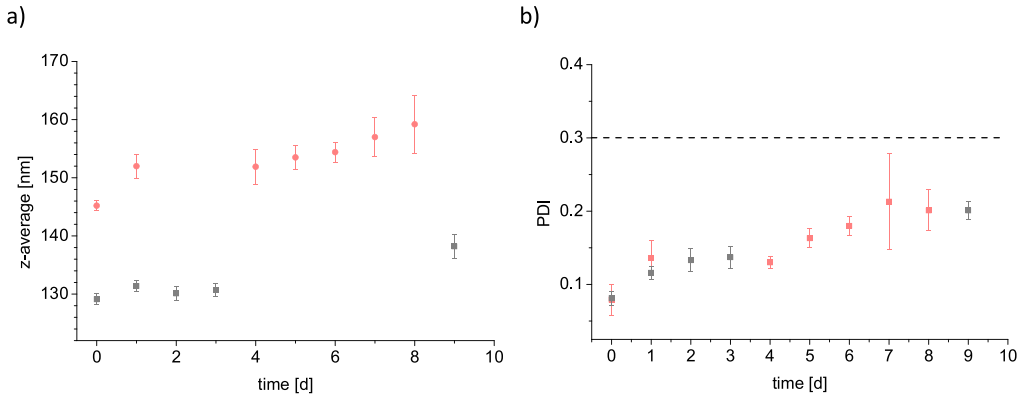

Fig. 4. Means of the diameters (z average) (a) and of PDI (b) of ULVs consisting of CER[AP]:CHOL:SA in buffer (pH = 10, grey) and in 10% DMSO in buffer (pH = 10, light red), dependent on storage time.

liposomes in 10% DMSO increased slightly to 159.2 ± 5.0 nm. During that time period, the polydispersity index (PDI) of the liposomes in DMSO increased to the same extend as for liposomes in buffer solution (see Fig. 4b).

In summary, it can be stated that the incorporation of DMSO caused an increased need of lipid per liposome. The higher inhomogeneity in the particle size distribution of the liposomes within eight days appears to be caused by the system itself and not by DMSO.

The leakage for liposomes in buffer at pH = 7 was not significantly different than for liposomes at pH 10 (see Table 4). The pH of 10 was used in order to check whether there is a strong pH dependence of the leakage which have to be considered by comparing the different model systems used. However, this was not the case as the leakage studies using SC ULVs with a DMSO concentration of 10% show significant but low leakages between 5 and 8% (Fig. 5a/b and Table 4) indicating a very low influence of DMSO on the structure of the liposomes at both pH values. By addition of DMSO in each concentration, there is an initial leakage that does not increase by the time. To cause such a leakage, the 6-CF molecule has to overcome the liposome membrane, which can be realized via pore formation or by destruction of the whole liposome as a result of solubilisation. In case of pore formation an initial leakage that increases by the time would be expected, as not the whole amount of 6-CF molecules would be released at a time. Consequently, this abrupt but not time dependent leakage at both pH values indicates a destruction of the liposomes due to solubilization of the lipids caused by DMSO.

The dependence of the leakage on the DMSO concentration is shown in Fig. 5b. The leakage increased from 5% (10% DMSO) via 13.6% (30% DMSO) to 60% (50% DMSO).

These results indicate that two aspects have to be taken into consideration: (i) Liposomes based on SC lipids are very stable because they cannot be completely destroyed by even 50% DMSO. In contrast to that, molecular dynamic simulations showed that phospholipid based liposomes could be destroyed by much lower DMSO concentrations (Hughes et al., 2012). (ii) The leakage caused by 10% of DMSO (8%) at pH 7 after 50 min is much lower than the leakage caused by 10% of urea (19.4%) under the same conditions (Mueller et al., 2016).

However, for a final conclusion, it also has to be considered that after addition of DMSO the solute concentration outside the vesicles changes. The so induced osmotic gradient is even higher, the higher the DMSO concentration is and might influence the vesicle stability as well. Consequently, especially at high DMSO concentrations of 50% or even 30% the observed leakage could also be induced by the osmotic gradient or a combination of this effect together with the interactions of DMSO.

Table 4
6-CF leakage [%] of the data presented in Fig. 4a and b.

pH	buffer	DMSO 10 %	DMSO 30 %	DMSO 50 %
10	0.5 ± 0.4	5.4 ± 1.6	13.6 ± 1.1	59.7 ± 1.4
7	1.4 ± 0.8	7.7 ± 0.8	–	–

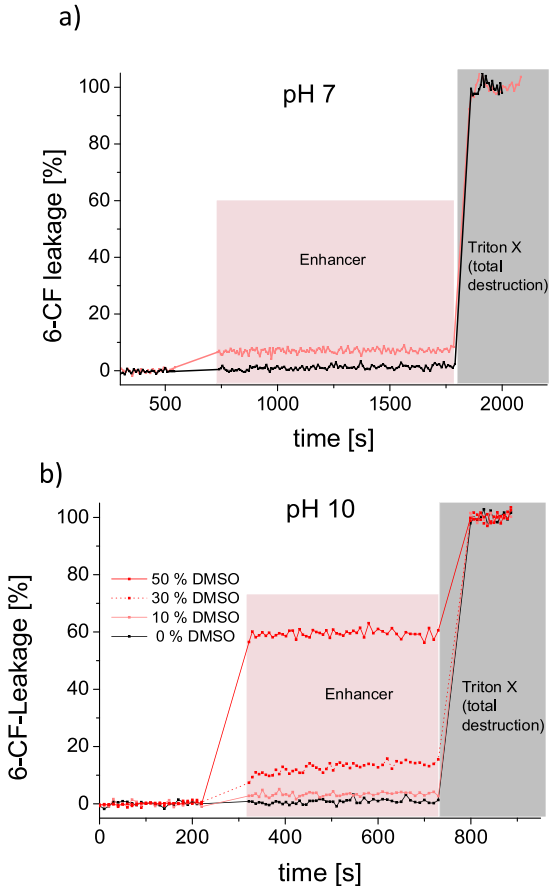

Fig. 5. a) Time dependent 6-CF leakage from ULVs consisting of CER [AP]:CHOL:SA in buffer (pH = 7) (grey) and after addition of 10% DMSO (light red). **b)** Time dependent 6-CF leakage from ULVs consisting of CER [AP]:CHOL:SA in buffer (pH = 10) in dependence of the DMSO concentration (0, 10, 30 and 50%).

5. Conclusions

Our studies show that DMSO in a concentration of 10% slightly interacts with SC model lipids. IR measurements show a reduction of

Table 5
Summary of the results obtained for the different hydrophilic penetration enhancer using the model system described in this paper and the supposed mechanism of the penetration enhancement (IR…infrared spectroscopy, NR…neutron reflectivity, HB…hydrogen bonds, PCS… photon correlation spectroscopy).

	Urea[a]	Taurine[a]	DMSO
IR (Multilayer)	Increase of the HB (amide-I)	No influence (Tendency: Increase of the HB (amide-I))	Decrease of the HB (amide-I)
IR (Oligolayer)	No influence	No influence	No influence (ν(CO) n.d.)
NR (Oligolayer)	No influence	No influence	Solubilization, Expansion of the head groups(30 %)
NR (Bilayer)	No influence	No influence	–
PCS (ULVs)	Coalescence	Incorporation into the head groups, coalescence	Incorporation into the head groups
Leakage (ULVs)	Pore formation	Pore formation	Slight solubilization
Supposed penetration enhancing mechanisms in SC	Pore formation in the SC lipid matrix, Accumulation in the corneocytes and increased water incorporation	Pore formation in the SC lipid¬ matrix, Accumulation in the corneocytes and increased water incorporation	Solubilization of SC lipids, Expansion of the head groups, Improved solubility for drugs and actives

[a] Müller et al. (2016).

the hydrogen bonds both of the C═O group of the amide and of the stearic acid. NR measurements on oligolayers indicate that these interactions in the range of the head groups have no influence on the lamellar repeating distance. Furthermore, neither an interaction of 10% DMSO with the lipid chains, nor an accumulation of DMSO in special areas of the bilayers could be observed.

Just for PCS measurements a slight increase of the liposome diameters has been detected. However, this is most probably reasoned by the incorporation of DMSO molecules into the head groups of the SC model lipids and a corresponding increased need of lipid per liposome to ensure the packing density of the liposomes. The stability of the liposomes in terms of size and particle size distribution was not affected by 10% DMSO in comparison to the buffer solution. As shown in Table 5, the very low leakage of 8% demonstrates that the influence of 10% DMSO on the integrity of the liposomes is very low and only a small part of the lipids could be solubilized. In contrast, a leakage of 19.4% was caused using solutions with 10% urea (Müller et al., 2016). The influence of DMSO on SC model systems used as well as its proposed penetration enhancement mechanism is summarized in Table 5 in comparison to urea and taurine, respectively. An increase in the DMSO concentration to 30% caused an increase in the thickness of the bilayers of the liposomes and in the total thickness of the lipid layers as shown by NR measurements. This increase in the thickness appears to be caused by an accumulation of the molecules of the medium in the head group region. Simultaneously, a part of the lipids is solubilized. However, the extend of solubilization is very low, since the leakage of 13.6% at pH 10 caused by 30% DMSO is just slightly higher than the leakage caused by 10% DMSO. Furthermore, no influence on the lipid chains could be observed.

The solution with 50% DMSO caused a distinct leakage of 60% indicating an extensive destruction of the lipid structure. Furthermore, IR measurements on multilayers show a higher reduction of the hydrogen bonds caused by 50% of DMSO compared to the solution with 10% of DMSO. However, neither a change in the hexagonal chain packing nor a reduction of the order of the lipid chains was caused by 50% DMSO. These results are in agreement with findings of Kwak and Lafleur, 2009. These authors reported that DMSO is causing a disordering and fluidization of the lipid chains by altering the interfacial H-bond network when DMSO was applied in concentration of 60%. Notman et al., 2007, obtained similar results using molecular dynamic simulations. They found that DMSO is accumulated in the headgroup region and decreases the lateral forces between the ceramide molecules.

Finally, the leakage results, especially for higher DMSO concentrations show more drastic effects of DMSO on the lipid structure than the other methods applied. This is mainly reasoned by the varying potential of the different model systems to interact with hydrophilic penetration enhancers. Although DMSO is able to penetrate into the lipid model mixtures, the interactions at the water/lipid interface are expected to be more distinct and decrease with increasing distance from this interface, as the DMSO concentration decreases along to the concentration gradient. Consequently, the model system with just one bilayer structure (liposomes) was expected to show the greatest effect, whereas the multilayer system with hundreds of bilayers revealed only a slight influence of DMSO. In addition, it also has to be considered that for leakage measurements the osmotic gradient has not been compensated, what might have caused or contributed to the great leakage as well.

In summary, the interactions of DMSO with SC model lipids are very low in concentrations of 10% and 30%, respectively. Since the lipid composition in native SC lipid matrix is far more complex than this model mixture, the results can not be directly transferred to the native SC lipid matrix. Based on the results of the present study, it can´t be excluded that the influence of DMSO on SC lipid mixtures composed of other lipid species, especially CERs, or on more complex mixtures, might be more pronounced than for the CER[AP] system. However, in combination with results from various studies concerning the influence of DMSO on the SC, the findings in this work support the assumption, that the enhancing effect of DMSO concerning the diffusion of relevant hydrophilic drugs and actives appears to be realized via the corneocytes. These results are in agreement with findings of Mendelsohn et al. (2006). They reported that DMSO treatment is influencing the keratin structure of the corneocytes by forming an extensive antiparallel ß-sheet structure in the keratin of the corneocytes.

Two publications recently published show that hydrophilic substances and cosmetic actives are able to diffuse easily into the corneocytes (Hussain et al., 2019a,b).

Declaration of Competing Interest

None.

Acknowledgement

This work is funded by the Deutsche Forschungsgemeinschaft (Project No. NE 427/30-1).

Appendix A. Supplementary data

Supplementary material related to this article can be found, in the online version, at doi:https://doi.org/10.1016/j.chemphyslip.2019.104816.

References

Allenby, A.C., Fletcher, J., Schock, C., Tees, T.F.S., 1969. The effect of heat, pH and organic solvents on the electrical impedance and permeability of excised human skin. Br. J. Dermatol. 81, 31–39.

Anigbogu, A.N.C., Williams, A.C., Barry, B.W., Edwards, H.G.M., 1995. Fourier-Transform Raman spectroscopy of interactions between the penetration enhancer dimethylsulfoxide and human Stratum corneum. Int. J. Pharm. 125, 265–282.

Barry, B.W., 1987. Mode of action of penetration enhancers in human skin. J. Control. Release 6, 85–97.

Blumenthal, R., Weinstein, J.N., Sharrow, S.O., Henkart, P., 1977. Liposome–lymphocyte interaction: saturable sites for transfer and intracellular release of liposome contents. Proc. Natl. Acad. Sci. U. S. A. 74, 5603–5607.

Boddé, H.E., van den Brink, I., Koerten, H.K., de Haan, F.H.N., 1991. Visualization of in vitro percutaneous penetration of mercuric chloride; transport through intercellular space versus cellular uptake through desmosomes. J. Control. Release 15, 227–236.

Born, M., Wolf, E., 2000. Principles of optics: electromagnetic theory of propagation, interference and diffraction of light. CUP Archive.

Bouwstra, J.A., Dubbelaar, F.E., Gooris, G.S., Ponec, M., 2000. The lipid organisation in the skin barrier. Acta Derm. Venereol. Suppl. 208, 23–30.

Coldman, M.F., Kalinovsky, T., Poulsen, B., 1971. The in vitro penetration of fluocinonide through human skin from different volumes of DMSO. Br. J. Dermatol. 85, 457–461.

de la Maza, A., Parra, J.L., 1996. Assembly properties of triton X-100/phosphatidylcholine aggregates during liposome solubilization. Colloid Polym. Sci. 274, 866–874.

de Jager, M.W., Gooris, G.S., Dolbnya, I.P., Bras, W., Ponec, M., Bouwstra, J.A., 2004. Novel lipid mixtures based on synthetic ceramides reproduce the unique stratum corneum lipid organization. J. Lipid Res. 45 (5), 923–932.

de Jager, M.W., Gooris, G.S., Ponec, M., Bouwstra, J.A., 2005. Lipid mixtures prepared with well-defined synthetic ceramides closely mimic the unique stratum corneum lipid phase behavior. J. Lipid Res. 46 (12), 2649–2656.

Dragicevic, N., Atkinson, J.P., Maibach, H.I., 2015. Chemical penetration enhancers: classification and mode of action. Percutaneous Penetration Enhancers Chemical Methods in Penetration Enhancement. Springer, pp. 11–27.

Elias, P.M., 1983. Epidermal lipids, barrier function, and desquamation. J. Invest. Dermatol. 80 (Suppl), 44s–49s.

Engelbrecht, T.N., Deme, B., Dobner, B., Neubert, R.H.H., 2012. Study of the influence of the penetration enhancer isopropyl myristate on the nanostructure of stratum corneum lipid model membranes using neutron diffraction and deuterium labelling. Skin Pharmacol. Physiol. 25 (4), 200–207.

Engelbrecht, T.N., Schroeter, A., Hauss, T., Neubert, R.H., 2011. Lipophilic penetration enhancers and their impact to the bilayer structure of stratum corneum lipid model membranes: neutron diffraction studies based on the example oleic acid. Biochim. Biophys. Acta 1808 (12), 2798–2806.

Guillard, E.C., Tfayli, A., Laugel, C., Baillet-Guffroy, A., 2009. Molecular interactions of penetration enhancers within ceramides organization: a FTIR approach. Eur. J. Pharm. Sci. 36, 192–199.

Hansch, C., Leo, A., Hoekman, D., 1995. Exploring QSAR – Hydrophobic, Electronic, and Steric Constants. American Chemical Society, Washington, DC, pp. 5.

Heavens, O.S., 1960. Optical properties of thin films. Rep. Prog. Phys. 23, 1.

Hikima, T., Maibach, H., 2006. Skin penetration flux and lag-time of steroids across hydrated and dehydrated human skin in vitro. Biol. Pharm. Bull. 29, 2270–2273.

Hughes, Z.E., Mark, A.E., Mancera, R.L., 2012. Molecular dynamics simulations of the interactions of DMSO with DPPC and DOPC phospholipid membranes. J. Phys. Chem. B 116, 11911–11923.

Hussain, H., Ziegler, J., Hause, G., Wohlrab, J., Neubert, R.H.H., 2019a. Free amino acids and urea derived from corneocytes of healthy, aged and diseased individuals. Skin Pharmacol. Physiol. 32, 94–100.

Hussain, H., Ziegler, J., Mrestani, Y., Neubert, R.H.H., 2019b. Diffusion of taurine into isolated corneocytes. Pharmazie 74, 340–344.

Kalbitz, J., Neubert, R., Wohlrab, W., 1996. Modulation of drug penetration into the skin. Pharmazie 51, 619–637.

Kessner, D., Kiselev, M., Dante, S., Hauss, T., Lersch, P., Wartewig, S., Neubert, R.H.H., 2008. Arrangement of ceramide [EOS] in a stratum corneum lipid model matrix: new aspects revealed by neutron diffraction studies. Eur. Biophys. J. 37, 989–999.

Kiselev, M.A., Ryabova, N.Y., Balagurov, A.M., Dante, S., Hauss, T., Zbytovska, J., Wartewig, S., Neubert, R.H., 2005. New insights into the structure and hydration of a stratum corneum lipid model membrane by neutron diffraction. Eur. Biophys. J. 34 (8), 1030–1040.

Kiselev, M.A., Ermakova, E.V., Gruzinov, A.Yu., Zabelin, A.V., 2007. Conformation of ceramide 6 molecules and chain-flip transitions in the lipid matrix of the outermost layer of mammalian skin, the Stratum corneum. Cryst. Rep. 52, 525–528.

Kwak, S., Lafleur, M., 2009. Effect of dimethylsulfoxide on the phase behavior of model stratum corneum lipid mixtures. Chem. Phys. Lipids 161, 11–21.

Lampe, M.A., Burlingame, A.L., Whitney, J., Williams, M.L., Brown, B.E., Roitman, E., Elias, P.M., 1983. Human stratum corneum lipids: characterization and regional variations. J. Lipid Res. 24, 120–130.

Law, S., Wertz, P.W., Swartzendruber, D.C., Squier, C.A., 1995. Regional variation in content, composition and organization of porcine epithelial barrier lipids revealed by thin-layer chromatography and transmission electron microscopy. Arch. Oral Biol. 40, 1085–1091.

Maibach, H.I., Feldmann, R.J., 1967. The effect of DMSO on percutaneous penetration of hydrocortisone and testosterone in man. Ann. N. Y. Acad. Sci. 141, 423–427.

Melnik, B.C., Hollmann, L., Erler, E., Verhoeven, B., Plewig, G., 1989. Microanalytical screening of all major stratum corneum lipids by sequential high-performance thin-layer chromatography. J. Invest. Dermatol. 92, 231–234.

Mendelsohn, R., Flach, C.R., Moore, D.J., 2006. Determination of molecular conformation and permeation in skin via IR spectroscopy, microscopy, and imaging. Biochim. Biophys. Acta 1758 (7), 923–933.

Mennicke, U., Salditt, T., 2002. Preparation of solid-supported lipid bilayers by spin-coating. Langmuir 18, 8172–8177.

Mueller, J., Schroeter, A., Steitz, A., Trapp, M., Neubert, R.H., 2016. Preparation of a new oligolamellar stratum corneum lipid model. Langmuir 32, 4673–4680.

Müller, J., Oliveira, J.S.L., Barker, R., Trapp, M., Schroeter, A., Brezesinski, G., Neubert, R.H.H., 2016. The effect of urea and taurine as hydrophilic penetration enhancers on stratum corneum lipid models. Biochim. Biophys. Acta 1858, 2006–2018.

Nishijo, J., Shiota, S., Mazima, K., Inoue, Y., Mizuno, H., Yoshida, J., 2000. Interactions of cyclodextrins with dipalmitoyl, distearoyl, and dimyristoyl phosphatidyl choline liposomes. A study by leakage of carboxyfluorescein in inner aqueous phase of unilamellar liposomes. Chem. Pharm. Bull. (Tokyo) 48, 48–52.

Norlen, L., 2001. Skin barrier structure and function: the single gel phase model. J. Invest. Dermatol. 117, 830–836.

Notman, R., Anwar, J., Briels, W.J., Noro, M.G., den Otter, W.K., 2008. Simulations of skin barrier function: free energies of hydrophobic and hydrophilic transmembrane pores in ceramide bilayers. Biophys. J. 95, 4763–4771.

Notman, R., den Otter, W.K., Noro, G.M., Briels, W.J., Anwar, J., 2007. The permeability enhancing mechanism of DMSO in ceramide bilayers simulated by molecular dynamics. Biophys. J. 93, 2056–2068.

Oertel, R.P., 1977. Protein conformational changes induced in human stratum corneum by organic sulfoxides: an infrared spectroscopic investigation. Biopolymers 16, 2329–2345.

Schmitt, T., Neubert, R.H.H., 2018. State of the art in stratum corneum research: the biophysical properties of ceramides. Chem. Phys. Lipids 216, 91–103.

Schroeter, A., Kessner, D., Kiselev, M.A., Hauß, T., Dante, S., Neubert, R.H.H., 2009a. Basic nanostructure of stratum corneum lipid matrices based on ceramides [EOS] and [AP]: a neutron diffraction study. Biophys. J. 97, 1104–1114.

Schroeter, A., Kiselev, M.A., Hauß, T., Dante, S., Neubert, R.H.H., 2009b. Evidence of free fatty acid interdigitation in stratum conreum model membranes based in ceramide [AP] by deuterium labelling. Biochim. Biophys. Acta 1788, 2194–2203.

Strobl, M., Steitz, R., Kreuzer, M., Rose, M., Herrlich, H., Mezei, F., Grunze, M., Dahint, R., 2011. BioRef: a versatile time-of-flight reflectometer for soft matter applications at Helmholtz-Zentrum Berlin. Rev. Sci. Instrum. 82, 055101–055109.

Talreja, P., Kasting, G., Kleene, N., Pickens, W., Wang, T.-F., 2001. Visualization of the lipid barrier and measurement of lipid pathlength in human stratum corneum. AAPS PharmSci 3, 48–56.

t'Kindt, R., Jorge, L., Dumont, E., Couturon, P., David, F., Sandra, P., Sandra, K., 2012. Profiling and characterizing skin ceramides using reversed-phase liquid chromatographyquadrupole time-of-flight mass spectrometry. Anal. Chem. 84, 403–411.

Torchilin, V.P., Weissig, V., 2003. Liposomes—A Practical Approach, 2nd edition. Oxford University Press, Oxford.

Trommer, H., Neubert, R.H.H., 2006. Overcoming the stratum corneum: the modulation of skin penetration. A review. Skin Pharmacol. Physiol. 19, 106–121.

van Well, A.A., 1992. Double-disk chopper for neutron time-of-flight experiments. Physica B Condens. Matter 180–181, 959–961.

Wertz, P.W., van den Bergh, B., 1998. The physical, chemical and functional properties of lipids in the skin and other biological barriers. Chem. Phys. Lipids 91, 85–96.

Williams, A.C., Barry, B.W., 2012. Penetration enhancers. Adv. Drug Deliv. Rev. 64, 128–137.

Zbytovska, J., 2006. New insights into the stratum corneum lipid membrane organisation; An X-ray and neutron scattering study. Dissertation. Mathematisch-Naturwissenschaftlich-Technischen Fakultät (Mathematisch-Naturwissenschaftlicher Bereich). Martin-Luther-Universität, Halle-Wittenberg, pp. 116.

Zbytovská, J., Kiselev, M.A., Funari, S.S., Garamus, V.M., Wartewig, S., Palát, K., Neubert, R., 2008. Influence of cholesterol on the structure of stratum corneum lipid model membrane. Colloids Surf. A Physicochem. Eng. Asp. 328, 90–99.

Zbytovska, J., Vavrova, K., Kiselev, M.A., Lessieur, P., Wartewig, S., Neubert, R.H.H., 2009. The effects of transdermal permeation enhancers on thermotropic phase behaviour of a stratum corneum lipid model. Colloids Surf. A Physicochem. Eng. Asp. 351 (1–3), 30–37.